A Level-Crossing Based QRS-Detection Algorithm for Wearable ECG Sensors

Nassim Ravanshad, *Student Member, IEEE*, Hamidreza Rezaee-Dehsorkh, *Student Member, IEEE*,
Reza Lotfi, *Member, IEEE*, and Yong Lian, *Fellow, IEEE*

Abstract—In this paper, an asynchronous analog-to-information conversion system is introduced for measuring the RR intervals of the electrocardiogram (ECG) signals. The system contains a modified level-crossing analog-to-digital converter and a novel algorithm for detecting the R-peaks from the level-crossing sampled data in a compressed volume of data. Simulated with MIT-BIH Arrhythmia Database, the proposed system delivers an average detection accuracy of 98.3%, a sensitivity of 98.89%, and a positive prediction of 99.4%. Synthesized in 0.13 μm CMOS technology with a 1.2 V supply voltage, the overall system consumes 622 nW with core area of 0.136 mm^2, which make it suitable for wearable wireless ECG sensors in body-sensor networks.

Index Terms—Analog-to-digital converter (ADC), asynchronous analog-to-information conversion system, level-crossing sampling, QRS detection, wearable electrocardiogram (ECG) monitoring devices.

I. INTRODUCTION

LEVEL-CROSSING sampling is getting popular in a wide class of low-power sensor–interface systems due to its simplicity and superior power efficiency. The activity-dependent nature of this sampling scheme, in which a new sample is taken only when a significant change occurs in the input-signal value, leads to a considerable performance improvement in the data acquisition systems when operating on sparse burst-like signals. The advantages of level-crossing sampling over traditional Nyquist sampling were first reported in [1], where its ability in data compression is demonstrated. The application of level-crossing sampling scheme to analog-to-digital converters (ADCs) also attracted much attention [2], [3]. Other systems utilizing the level-crossing sampling has been reported in the past decade including speech [3]–[5], ultrasound [6], accelerometer [7], and biomedical signal acquisition [8]. Utilizing level-crossing sampling for creating an event-driven system is considered by a growing number of researches, some focus on developing complete level-crossing-based systems [including

ADC, processor, and digital-to-analog converter (DAC)] [9], [10], others try to improve the efficiency of the system for specific applications [5], [7], [8], [11], [12], and yet others develop circuit techniques for low-cost circuit implementation of level-crossing-based systems [13]–[15].

In this paper, we focus on developing level-crossing-based QRS detector for cardiac monitoring devices. Electrical activity of the heart, which is detectable by placing the electrodes at the outer surface of the skin, can be recorded by the electrocardiograph device. The electrocardiogram (ECG) signal provides valuable information about the rate and regularity of the heart beats, which can be used in diagnosis of cardiac diseases. The most significant feature of the ECG signal is the QRS complex, the peak of which is specified as R-peak [16]. The RR interval, which is the time interval between two consecutive R peaks, can be used to detect irregularities in the heart normal operation, called arrhythmia. Many QRS-detection algorithms were proposed and widely studied for decades. The basic techniques are based on the amplitude, i.e., first derivative or first and second derivatives of the signal [17], [18]. More complicated algorithms such as wavelet-based QRS detection, filter-bank methods, neural network approaches, mathematical morphology, and others are reviewed and compared in [19]. Despite the high functionality of these methods, most of them need complex computations that restrict their use in the body sensor networks (BSNs). The ambulatory monitoring in BSN usually uses wearable devices to record the signals continuously for a long period of time. Such systems have to be designed with minimum size, complexity, and power consumption.

Several solutions have been presented in order to achieve these goals, most of which are aimed to extract the desired characteristics of the signal by using a compressed number of samples. The suggested methods such as wavelet compression and compressed sensing suffer from large amount of acquired data and the complex digital postprocessing for data reconstruction, respectively, and therefore are not applicable for wearable devices, especially for self-powered devices in BSN. Asynchronous level-crossing sampling scheme is an alternative approach for this purpose, which meets both targets of data compression and feature extraction simultaneously [7], [8]. Under the scheme, the sampling rate is directly proportional to the activity of the input signal and no power is wasted for sampling, converting, and processing the useless data in the inactive parts of the signal. This is well suited for ECG signal due to its sparse and burst-like nature. However, there are limited works studying the QRS detection using level-crossing sampled data [8], [11], [20].
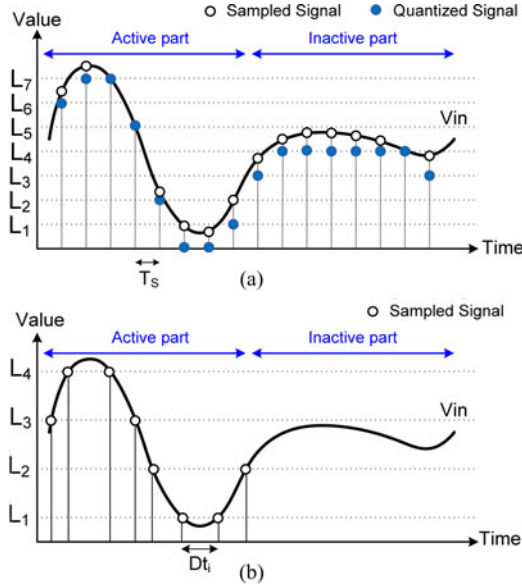
Fig. 1. Different sampling schemes with the same number of samples in the active part of the signal: (a) regular synchronous sampling and (b) level-crossing sampling.

In this paper, a novel algorithm for extracting the RR intervals from the output data of the level-crossing-based ADC (LC-ADC) is proposed. It employs special features of level-crossing sampling in order to achieve improved power efficiency as well as detection accuracy. The system performance is evaluated using all recordings of the MIT-BIH Arrhythmia Database [21]–[23].

The rest of the paper is organized as follows: Section II includes a brief description about the basics of the LC-ADC operation. The proposed QRS-detection algorithm is introduced in Section III. The evaluation of the algorithm is presented in Section IV, followed by performance comparison in Section V. Finally, the concluding remarks are presented in Section VI.

II. LEVEL-CROSSING ADC

The illustrations of the synchronous and level-crossing sampling are shown in Fig. 1. The synchronous sampling is based on a reference clock with a constant period of T_S and so the time intervals between the samples are constant. The level-crossing sampling, on the other hand, is an irregular or asynchronous sampling method. It divides the amplitude into $2^M - 1$ quantization levels, indicated as dotted lines in Fig. 1(b), in which M is the ADC physical number-of-bits or resolution. A sample is taken only when the input signal crosses one of these quantization levels [2].

Using the level-crossing sampling, the conversion process and so the operation of the LC-ADC is dependent on the amplitude change in the input signal and so the sampling rate is proportional to the activity of the input signal. This property may lead to advantages in using the LC-ADC for two types of signals. The first type is the sparse signals that are approximately constant in most of the times and active in small time intervals such as speech, pressure, temperature, heart, and neural signals. In these types of signals, when the signal has small variations

such that no level-crossing happens, the circuit is in the sleep mode and no sample is taken. No extra power is wasted for data conversion in the intervals with little useful data and the average sampling rate can be reduced that improves the system efficiency. The other type of signals is burst-like signals such as ECG, electroencephalogram (EEG), and electromyogram (EMG). Unlike the conventional synchronous ADCs, the accuracy of the LC-ADC is not limited by using limited number of the quantization levels. In the applications with burst-like signals, the power efficiency can be improved by using smaller hardware number of bits, which results in lower data rate and hardware complexity [3]. In the example shown in Fig. 1, the number of samples taken in the active part is the same as in the inactive part for a fixed interval under synchronous sampling scheme while level-crossing sampling takes much less samples in the inactive region. Since the ECG signal is both sparse and burst-like, it can benefit from level-crossing sampling.

Unlike the synchronous sampling, samples in the level-crossing sampling are unevenly distributed. Faster the input signal changes, closer the samples. Therefore, in addition to the value of the signal, the sampling instants should also be recorded by the LC-ADC. Several methods are presented for recording and processing the nonuniform sampled data coming from an LC-ADC. In order to transport and store these data by using a common synchronous system, the time intervals between the samples (Dt_i) can be quantized and represented with a limited number of bits [3]. Due to the fact that the values of the samples are exactly known and the sampling instants are quantized, the LC-ADC operation in this situation is the dual operation of a synchronous ADC, in which the sampling instants are exactly known and the data values are quantized. In order to measure the time interval between two adjacent samples, a local timer can be used. This timer can be simply a counter with a constant period of T_{Timer} or a more complicated time-to-digital converter (TDC). Unlike the synchronous analog-to-digital conversion, in level-crossing ADC, no inherent noise is added to the data values due to the limited number of quantization levels. The limited resolution of the timer is the factor that may reduce the accuracy of the ADC.

Irregular level-crossing samples of value and time can be processed using asynchronous signal processing methods [24], which is the method used in this paper for detecting the QRS complexes from the ECG signal. In this method, no additional circuitry is needed to convert the nonuniform sampled data to uniform ones as in [2] and no special continuous-time digital signal processor is needed to be designed as in [9].

III. QRS-DETECTION SYSTEM

A traditional QRS-detection system includes electrodes, low-noise amplifier, filter, variable-gain amplifier, ADC, and processing unit. In this section, we present a new approach for QRS detection that is based on asynchronous level-crossing ADC and nonuniformly spaced data processing. It is shown that by using this system, the processing data volume can be reduced considerably that may result in lower power consumption, especially for wireless transmission. Also the proposed
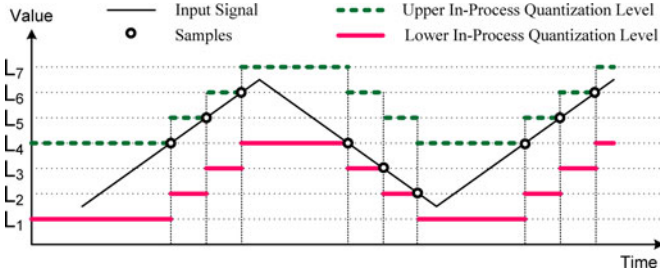
Fig. 2. Operation of the increased-gap LC-ADC: $k = 3$ LSB.

system significantly improves detection accuracy compared to the previous works that use LC-ADC for QRS detection.

A. Exploiting LC-ADC for QRS Detection

Detecting the QRS complex is challenged by appearance of various noise sources, such as muscles' contraction, power-line interference, baseline drift due to respiration, electrode contact noise, and motion artifact, especially in the case of wearable devices. Also other components of the signals, such as large P and T waves may destroy the detection process. In addition, the basic morphological feature of the QRS complex varies from patient to patient. Therefore, almost all the QRS-detection algorithms use some kinds of filtering to attenuate the unwanted parts of the signal, which can be implemented both in the analog domain (before the ADC) or digital domain (after the ADC and before the detection algorithm). In order to realize this filter in the analog domain with sufficient linearity, a narrow-band high-order bandpass filter is needed (5–15 Hz [25]), which cannot be implemented without increasing power consumption. Implementing the filter in the digital domain also burden extra computation and so power consumption to the system. It will be shown in the following that by using an LC-ADC one can simply omit most of the undesired noises and even signals with the amplitude less than a specified value. Using this property, a simple algorithm can be utilized to detect the QRS complex without using any additional circuitry or computation for excess filtering. There are just few works that mentioned the QRS detection by using the level-crossing samples [8], [11], in which just the activity-decrement property of the level-crossing sampling is considered. Pre-ADC filtering and adaptive-resolution techniques are used in [8] to enhance the detection performance at the expense of higher complexity and power consumption.

In order to explain the idea, it is necessary to understand the basic operation of LC-ADC, which is illustrated in Fig. 2. The LC-ADC produces the output based on a pair of in-process quantization levels, which should be specified and stored in two registers. The input signal should always be surrounded by these two quantization levels. Whenever the input signal leaves the gap between the two in-process quantization levels, the values of these levels increase or decrease by one least-significant bit (LSB) approaching the input signal. The LSB value is defined as follows:
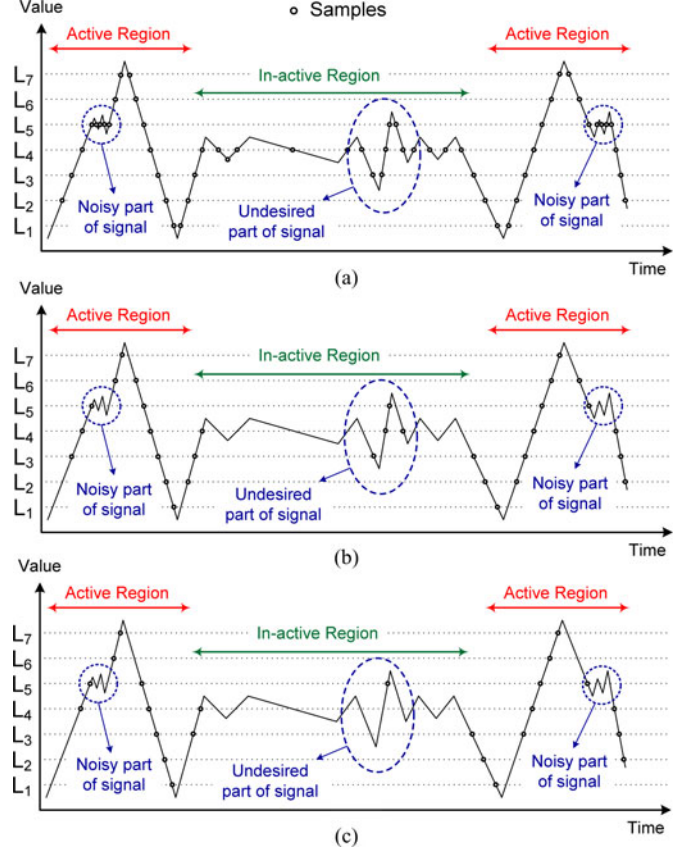
$$\text{LSB} = \frac{2A_{FS}}{2^M} \qquad (1)$$

Fig. 3. Effect of the increasing the gap between the two in-process quantization (k) on level-crossing sampling: (a) $k = 1$ LSB, (b) $k = 2$ LSB, and (c) $k = 3$ LSB.

where A_{FS} is the ADC input voltage amplitude range and M is the ADC resolution. Then, the new quantization levels are compared with the input signal again. This means that if the input signal is greater than the upper level, both levels are increased by 1 LSB and if the input signal is less than the lower level, both levels are decreased by 1 LSB. When the ADC starts operating, this process is performed repeatedly until the input signal is surrounded by the in-process quantization levels. Therefore, the LC-ADC may need an initial time to settle to the proper operation.

The gap between the two in-process quantization levels (denoted with k) is conventionally selected to be equal to 1 LSB, not to miss any level-crossing. In the situation of $k = 1$ LSB, as shown in Fig. 3(a), if the input signal experiences noise at the level-crossing point, it generates multiple crossings, i.e., there are too many un-wanted output samples that do not contain any useful information. In order to avoid such a problem, one way is to increase the k value to more than 1 LSB. Fig. 2 shows an example of $k = 3$ LSB. As it can be observed from this figure, samples are taken only when the signal changes more than 1 LSB at the same direction or $k-1$ LSB at the opposite direction. Under such a sampling scheme, as shown in Fig. 3(b) and (c), with every changing of direction in the input signal from rising to falling and vice versa, $k-1$ level-crossings are skipped and the signals with the amplitude of less than k LSB do not appear
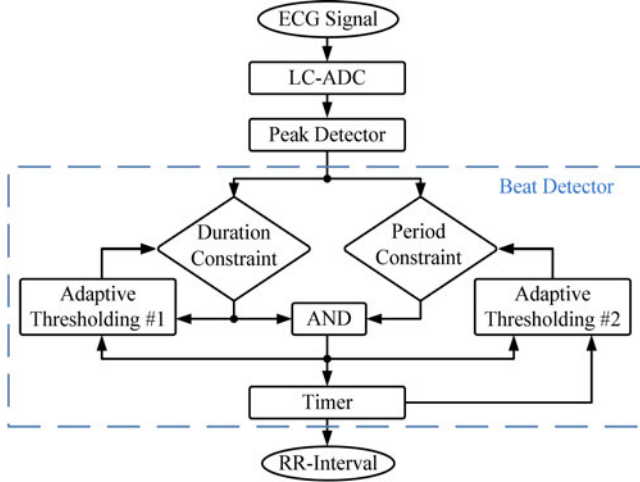
Fig. 4. Flowchart of the algorithm operation.

in the output. The benefits of the scheme are reduced sample points as well as noise filtering.

Different values of k can be applied to the ADC simply by loading the proper values into the registers that holds the values of the in-process quantization levels, at the startup. Therefore, no additional circuitry or complicated processes are needed to apply the selected k to the ADC or even change the value of k during the system operation.

B. QRS Detection Using Level-Crossing Samples

The main drawback of the level-crossing sampling method is that the subsequent signal processing needs to be done on nonuniformly sampled data comes from an LC-ADC. Complicated digital signal processing techniques are essential in order to apply the conventional QRS-detection algorithms to the asynchronous level-crossing sampled data. This may completely destroy the advantage of LC-ADC. In previous works that study the QRS detection using level-crossing sampled data, they either use amplitude thresholding [8] or convert nonuniform samples to uniform ones [11]. For amplitude thresholding, the large baseline wandering or sudden amplitude change in the signal, such as high R-peak or PVC (premature ventricular contraction), affect the accuracy of QRS detection. For nonuniform to uniform conversion [11], it requires extra conversion circuit or algorithm in addition to QRS-detection algorithm, which is not power efficient. As it is shown in the following, a simple but accurate QRS-detection algorithm can be developed that processes nonuniformly sampled data from an LC-ADC.

The flowchart of the proposed algorithm is shown in Fig. 4. As the first step, the ECG signal is passed through the LC-ADC. The block-diagram of the LC-ADC, including a sample of the input and output signals is shown in Fig. 5. The LC-ADC provides three signals at the output: a 2-bit signal representing the change of each sample value from the previous one (DV_i) {1 LSB ("01"), $k - 1$ LSB ("00"), -1 LSB ("10"), $-k + 1$ LSB ("11")}, a token signal to indicate the sampling occurrence and an 11-bit signal representing the time interval between the current sample and the previous one (Dt_i). The algorithm does not use the
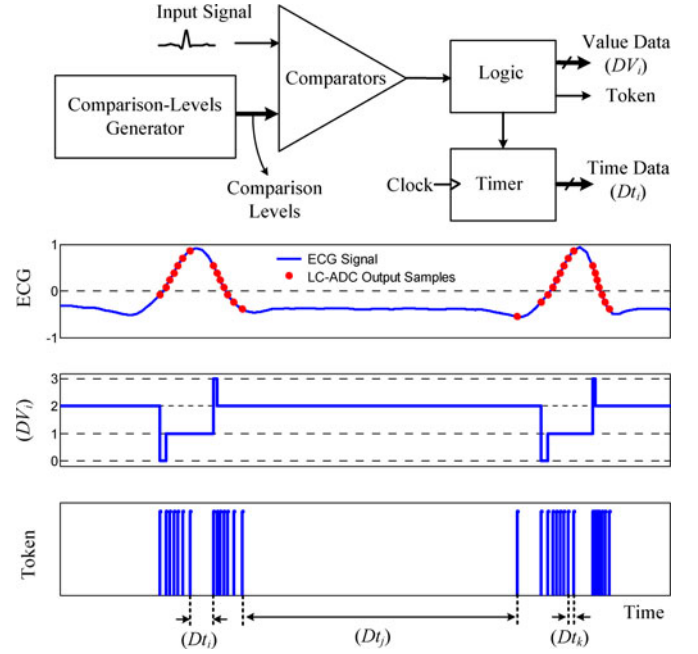

Fig. 5. Block diagram of the LC-ADC, including samples of the input and output signals.

value of the signal, but the change in the direction of the signal (up or down), which helps to detect the peaks. The second step is to detect the peaks of the signal that can be done by finding out that the DV_i value of the current sample is matched with "00" or "11" values.

The final step of the algorithm, which is the main one, is to find out whether this peak is an R-peak or not. The fundamental of this part of the algorithm is almost similar to the derivative-based algorithms. In the derivative based algorithms [16], as the time period of the sampling is constant, the difference between the values of consecutive samples represents the gradient of the input signal at each moment. For the level-crossing sampled data, the difference between the amplitude of consecutive samples is constant and so the time interval between two consecutive samples can be a representation of the input signal gradient. Smaller the time interval, larger the gradient of the input signal. Using this property, in the proposed algorithm, the time intervals (Dt_i) of a constant window of level-crossings (W level-crossing, which means $W - k + 1$ sample) around the detected peak is stored. The sum of the stored time intervals (dur) can be a representation of the spike duration that can be used to recognize the R-peaks:

$$\text{dur}(P) = \sum_{i=P-\left[\frac{W}{2}\right]}^{P+\left[\frac{W}{2}\right]-k+j} Dt_i, \qquad j = \begin{cases} 0, & \text{even } W \\ 1, & \text{odd } W \end{cases} \quad (2)$$

where P is the index of the sample in which the peak is detected and [x] represents the largest integer that is less than or equal to x.

The detection of a QRS complex is completed by comparing dur with a threshold value (TH_1). If dur is less than TH_1, which means that the duration of the spike is short enough and the
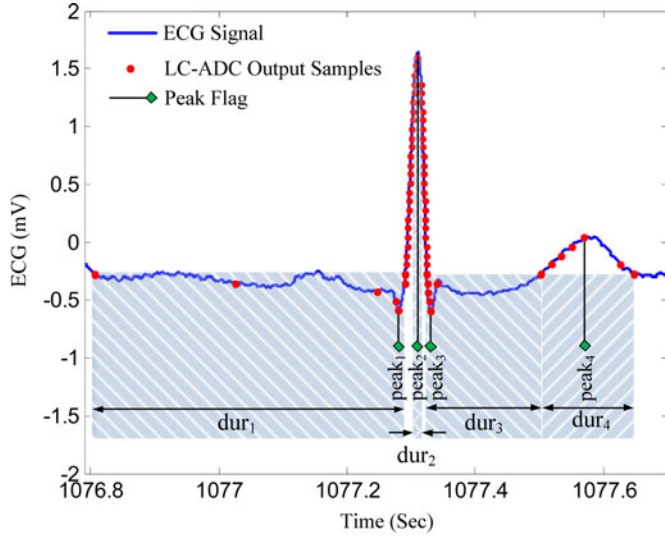
Fig. 6. Basics of operation of the proposed QRS-detection algorithm.

variation of the spike is fast enough, the peak can be declared as an R-peak. The operation of this method on a real ECG signal is shown in Fig. 6, which is a section cut of the Tape 103 of MIT-BIH Arrhythmia Database. The value of k is equal to 4 LSBs in this example. The signal has 4 peaks in this time interval and the values of dur are shown for $W = 9$. As it can be seen, the dur value for the R-peak is much smaller than the three other peaks.

As the slope of the R-waves and also the amplitude of the QRS complex varies from patient to patient and also over time, the range of dur values can be changed. Therefore, in order to reduce the sensitivity of the algorithm to the threshold value, TH_1 is tuned adaptively [26] during the algorithm operation using the following algorithm. This algorithm has three variables (SP, NP, and TH_1), which are initially set and adaptively updated by the algorithm, and two coefficients ($coeff_1$ and $coeff_2$), which are constant during the operation. SP is the running estimate of the dur value for the signal R-waves and NP is the running estimate of the dur value for the noise (not R-wave) peaks. If the detected peak is decided to be an R-peak

$$SP = SP - [coeff_1 \times (SP - dur)] \qquad (3)$$

otherwise,

$$NP = NP - [coeff_1 \times (NP - dur)] \qquad (4)$$

and for each detected peak the value of TH_1 is updated using

$$TH_1 = SP + [coeff_2 \times (NP - SP)]. \qquad (5)$$

The values of the $coeff_1$ and $coeff_2$ are both selected to be 0.25 and so the [coeff. x] terms of the aforementioned equations can be simply implemented by ignoring the two LSB bits without using an additional multiplier.

To avoid false QRS detection due to fast high T-waves, a dead-time zone is set up adaptively in order to reject any QRS detection too close to the previous one. In order to measure the RR intervals, either a local timer can be used or the time interval can be calculated by summing the Dt_i values. This part

of the algorithm can be realized by comparing the time interval between the current sample and the previous R-peak (ΔT_{Beat}) with a threshold (TH_2). The value of TH_2 is selected to be half of the average period of the beats (PoB). The PoB value is initially set and whenever an R-peak is detected, its value is updated adaptively using the following equation:

$$PoB = PoB - [coeff_3 \cdot (PoB - \Delta T_{Beat})]. \qquad (6)$$

The value of $coeff_3$ is selected to be 0.125 in order to simplify the implementation of [$coeff_3. x$] by just ignoring the three LSB bits. Therefore, all the coefficients are selected such that all the multiplications can be implemented using truncation. In order to prevent the algorithm from failure at the presence of a period of missed beats (e.g., in Tape 203 at around 1490 s), there should be a specified upper bound for PoB. An upper bound of 1 s is selected in this design.

In summary, the proposed algorithm detects the QRS complexes from the level-crossing sampled data by making use of special features embedded in the level-crossing samples, i.e., gradient and the time intervals between the samples. No additional circuitry is needed to convert the nonuniformly sampled data to uniform ones. The QRS detector fully benefits from the asynchronous operation of the LC-ADC and its data compression capability.

As it is obvious from the nature of the algorithm, in order to have a well-operated algorithm, minimum of W level-crossings should be captured by the LC-ADC from the R-wave. The number of the samples taken from the R-wave is directly related to the resolution of the LC-ADC (M). In order to find out the desired value of M for the QRS detection, the 48 half-hour-recorded ECG signals of the MIT-BIH Arrhythmia Database are applied to an LC-ADC that is modeled in MATLAB with various values of M and k. In order to have sufficient samples in the case of large values of M, linear interpolation is utilized to increase the sampling rate of the recordings of the MIT-BIH Arrhythmia Database by 16 times before applying to the LC-ADC. Using the LC-ADC output data, the possible locations of the beats are estimated utilizing simple peak detection and the numbers of missed beats are measured using beat-by-beat comparison [27]. The ratio of these values over the total number of beats (109428 beats in total) is calculated and plotted in Fig. 7(a) versus k for different values of M. To keep the missed beats within 0.05%, M should be greater than 7 bits for $k \geq 3$ LSB. Fig. 7(b) reveals the average sampling frequency of the entire 48 half-hour signals of the MIT-BIH Arrhythmia Database for the same values of M and k. It is obvious that 7-bit LC-ADC achieves much lower average sampling frequency at the same k values compared to its 8-bit counterpart. Furthermore, as mentioned in Section III-A and shown in Fig. 3(a), the cases of $k = 1$ LSB are not acceptable because the average sampling frequency is very sensitive to noise in these cases. The best design points are $\{M = 7, k = 2, 3, 4\}$ and $\{M = 6, k = 2\}$. Although the case $\{M = 6, k = 2\}$ has the lowest average sampling frequency, the samples at the active portions of the ECG signal is too sparse in this case, especially for low-amplitude signals, which affects the accuracy of QRS detection. Therefore, since higher values of k are preferred because of the noise immunity and lower average
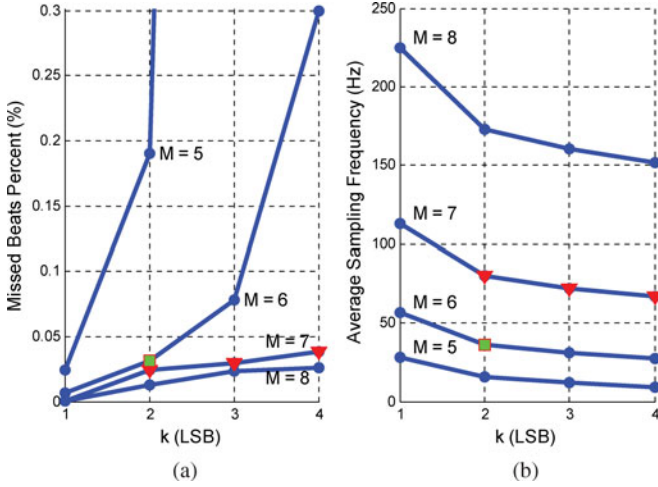
Fig. 7. Test results of the LC-ADC operation on the MIT-BIH Arrhythmia Database recordings.
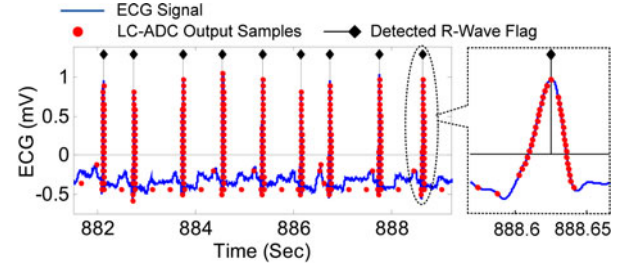

Fig. 8. Detection of the QRS using Tape 100 of MIT-BIH Arrhythmia Database with a standard ECG waveform and a zoom-in segment to show the exact location of the flags.

Fig. 9. Detection of the QRS using Tape 105 of MIT-BIH Arrhythmia Database: [(a) and (b)] baseline wander and (c) severe noises.

sampling frequency, the case $\{M = 7, k = 4\}$ can be a preferred design point. The average sampling frequency, over the entire database, is about 67 Hz in this case. This value is much less than the sampling frequency used by regular sampling systems, which is about 200–600 Hz (360 Hz for MIT database). Based on the maximum gradient of the input signals, a counter with the clock frequency of 5.76 kHz is used as the timer. It should also be mentioned that, since the minimum time interval between two consecutive samples is large enough (more than 0.5 ms), the algorithm can process the data and make decision before the next sample is captured. Therefore, no conflict is happened for processing close peaks. Also, based on the maximum time interval between consecutive samples, an 11-bit counter is used as the timer. If the timer reaches its maximum value before the next level-crossing, an extra sample is recorded to the output of the ADC. Although this sample does not represent a level-crossing and may contain k LSB error, it does not affect the detection algorithm because it is located in the inactive portion of the signal.

The best performance of the QRS detector is obtained for $W = 9$ by tuning the performance over MIT-BIH Arrhythmia Database. Using $W = 9$ and based on (2), just six samples are used for each beat evaluation. Based on (2), in the case of $k = 4$ and $W = 9$, the detection of the R-peaks is delayed by two samples. Simulation shows that this delay is less than 0.17 s for all the records of MIT-BIH Arrhythmia Database and the mean value of the delay is about 0.012 s, which are portions of the duration of the QRS complex. These values are at the order of the delay reported by other QRS-detection algorithms that is, for example, equal to half of the maximum possible duration of the normal QRS complex [16].

IV. PERFORMANCE EVALUATION

The proposed QRS detector is modeled and simulated in MATLAB. In order to evaluate the system functionality, the first channels of the 48 half-hour ECG recordings of MIT-BIH Arrhythmia Database are used. The signals are passed through
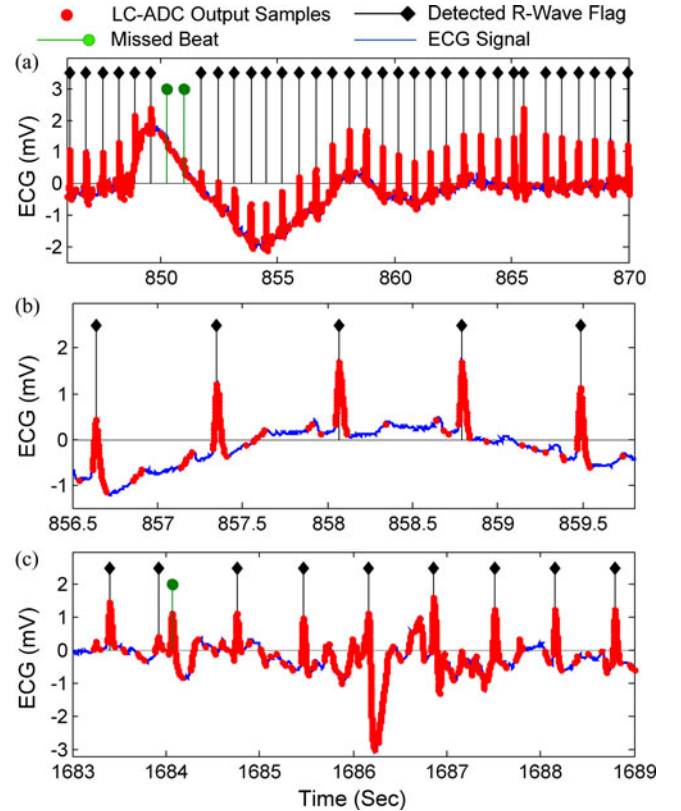
a 7-bit LC-ADC with $k = 4$ LSB and a 10 mV full-scale input range and then evaluated by the proposed algorithm. The performance of the algorithm, dealing with different abnormal ECG signals, is shown in Figs. 8–10.

In Fig. 8, a detection example of the QRS using Tape 100 and a zoom-in segment of this tape are shown. As it can be seen, nearly all the samples are taken from the QRS regions and no power is wasted to sample the silent parts of the signal with small variations. Fig. 9 shows the performance of the algorithm under the presence of the artifact using Tape 105. Fig. 10(a) and (b) demonstrates the handling of large P or T waves and irregular ECG signals, respectively. From all examples, it can be seen that the proposed system correctly detects the QRS complexes of the ECG signal, even under the presence of baseline drift, severe noise, large P or T waves, and irregular ECG waveform.

Fig. 10. Detection of the QRS using MIT-BIH Arrhythmia Database: (a) Tape 117: Large P or T waves, (b) Tape 200: Irregular ECG waveform.

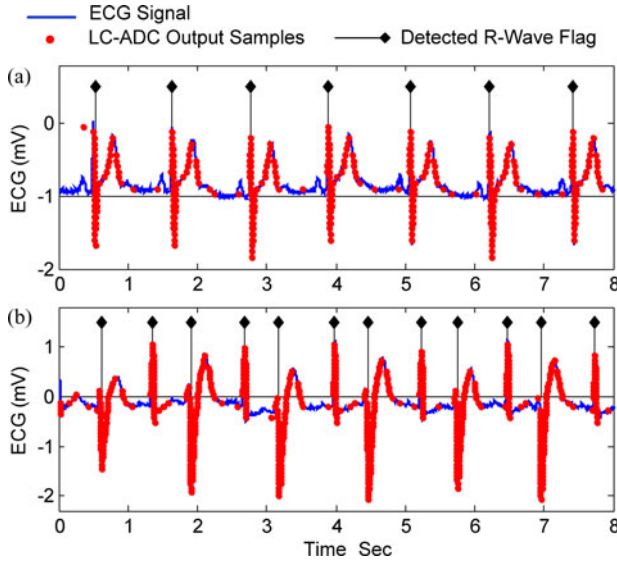In order to evaluate the performance of the QRS-detection algorithm, the numbers of failings to detect an R-peak (false negative or FN) and false beat detection (false positive or FP) are calculated for all 48 tapes under investigation using the standard of [27]. The results are reported in Table I. Using these values, three other parameters of sensitivity (Se), positive prediction ($+P$), and detection error rate (DER) are calculated and reported, which are defined as follows:

$$Se = \frac{TP}{TP + FN} \tag{7}$$

$$+P = \frac{TP}{TP + FP} \tag{8}$$

$$DER = \frac{FP + FN}{Total\ Beat} \tag{9}$$

in which true positive (TP) means the number of truly detected beats [27]. Based on the results of Table I, a detection error of 1.71% is obtained against the recordings of the MIT-BIH Arrhythmia Database. This performance is comparable to the current QRS-detection algorithms, all achieved at very large amount of sampled data, using complicated pre/post ADC filtering and complicated detection algorithms.

As it can be seen in Table I, there are just a few tapes (such as 203, 207, 213, and 222) in which almost large values are obtained for FN and/or FP characteristics. As shown in Fig. 11(a), Tape 203 suffers from high-amplitude, high-frequency noise. Therefore, as no filtering is used in the system and all the noises cannot be removed with the selected value of k, some noises are detected as beat. Moreover, detecting a noise signal as a beat just before an actual beat signal, causes missing the actual beat because of the period constraint and so couples of FP and FN are created. The constant value of k is tuned to reach the best result over the entire database, which also contains some very low-amplitude signals such as Tapes 222 and 232. Therefore, the value of k cannot be increased. This issue can be resolved

No.	Tape	Total Beat	FN	FP	Se (%)	+P (%)	DER (%)
1	100	2273	0	0	100	100	0
2	101	1865	4	8	99.79	99.57	0.64
3	102	2187	0	0	100	100	0
4	103	2084	0	0	100	100	0
5	104	2229	22	82	99.01	96.42	4.67
6	105	2572	41	63	98.41	97.57	4.04
7	106	2027	15	4	99.26	99.80	0.94
8	107	2137	4	2	99.81	99.91	0.28
9	108	1763	76	21	95.69	98.77	5.50
10	109	2532	3	3	99.88	99.88	0.24
11	111	2124	1	0	99.95	100	0.05
12	112	2539	15	1	99.41	99.96	0.63
13	113	1795	3	0	99.83	100	0.17
14	114	1879	22	4	98.83	99.79	1.38
15	115	1953	0	0	100	100	0
16	116	2412	22	6	99.09	99.75	1.16
17	117	1535	1	1	99.93	99.93	0.13
18	118	2278	22	36	99.03	98.43	2.55
19	119	1987	1	1	99.95	99.95	0.10
20	121	1863	4	1	99.79	99.95	0.27
21	122	2476	1	1	99.96	99.96	0.08
22	123	1518	0	0	100	100	0
23	124	1619	1	1	99.94	99.94	0.12
24	200	2601	45	71	98.27	97.30	4.46
25	201	1963	67	0	96.59	100	3.41
26	202	2136	21	1	99.02	99.95	1.03
27	203	2980	108	154	96.38	94.91	8.79
28	205	2656	13	2	99.51	99.92	0.56
29	207	1794	141	11	92.14	99.34	8.47
30	208	2955	49	32	98.34	98.91	2.74
31	209	3005	11	18	99.63	99.40	0.97
32	210	2650	58	20	97.81	99.23	2.94
33	212	2748	10	13	99.64	99.53	0.84
34	213	3251	104	4	96.80	99.87	3.32
35	214	2262	8	8	99.65	99.65	0.71
36	215	3363	3	7	99.91	99.79	0.30
37	217	2208	11	2	99.50	99.91	0.59
38	219	2154	13	0	99.40	100	0.60
39	220	2048	2	1	99.90	99.95	0.15
40	221	2427	5	5	99.79	99.79	0.41
41	222	2483	198	3	92.03	99.87	8.10*
42	223	2605	3	1	99.88	99.96	0.15
43	228	2053	21	39	98.98	98.12	2.92
44	230	2256	10	6	99.56	99.73	0.71
45	231	1571	1	5	99.94	99.68	0.38
46	232	1780	46	2	97.42	99.88	2.70
47	233	3079	9	10	99.71	99.68	0.62
48	234	2753	1	1	99.96	99.96	0.07
	Total	109428	1216	651	98.89	99.40	1.71

* 2% after amplitude adjustment.

by filtering the input signal or tuning the value of k based on the amplitude of the input signal.

In just three specific parts of Tape 207, a part of which is shown in Fig. 11(b), the input signal is messy and contains abnormal beats with large duration. It seems that for such a signal, the value of TH_2 should be updated at these specific parts of

TABLE II
COMPARISON OF THE PROPOSED ALGORITHM WITH ONE USED IN [8]

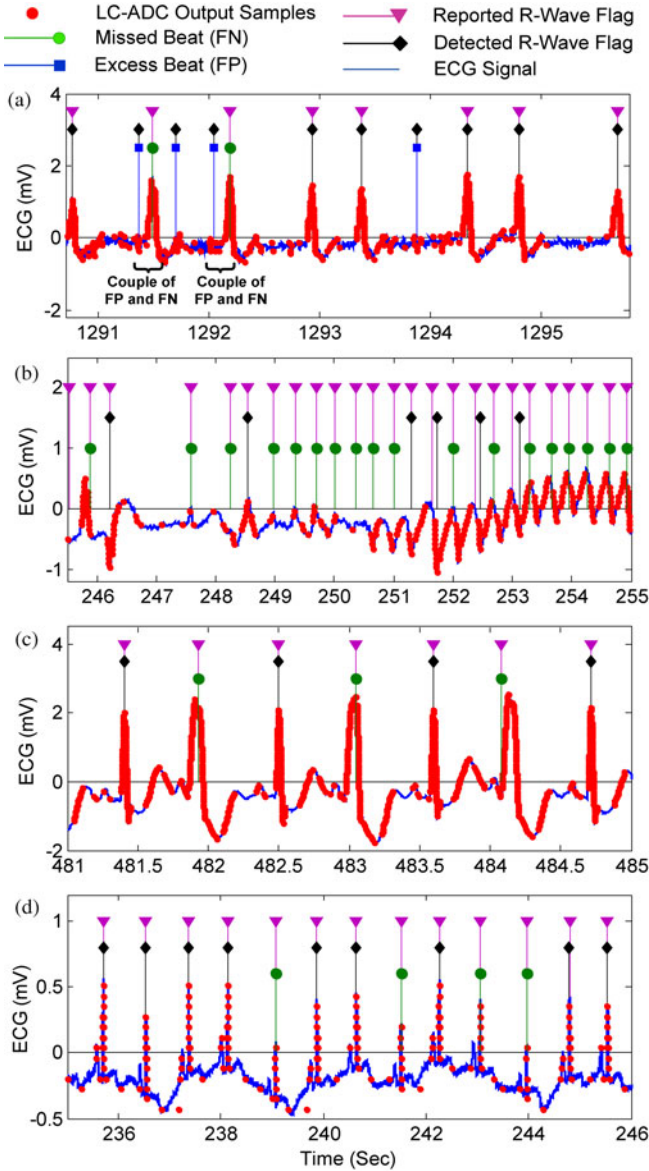| Tape	100	105	117	118	222
DER (%) [8]	0	7.73	69	0.79	39.6
DER (%) [This Work]	0	4.04	0.13	2.55	8.1

Fig. 11.   Detection of the QRS using MIT-BIH Arrhythmia Database: (a) Tape 203: sever noise results in couples of FP and FN, (b) Tape 207: missing beats due to messy input signal and abnormal beats with large duration, (c) Tape 213: missing beats due to abnormal beats with large duration, and (d) Tape 222: missing beats due to the lack of enough samples.

the signal. There are similar situations in some specific parts of Tape 213, which is shown in Fig. 11(c). Such a situation in which a couple of beats are missed due to thresholds' misalignment, can be resolved by using a conventional search-back technique [26], at the expence of more complexity.

The other factor that affects the performance of the proposed algorithm is large variations in signal amplitude, e.g., from a quarter of the full-scale to the full-scale. Actually the amplitude values of 97.9% of tapes are less than 80% of the full-scale range. Among them, about 50% are less than 50% of the full-scale range. There are also some signals such as Tapes 222 and 232, the amplitude values are just around a quarter of the full-scale range. Since the LC-ADC specifications (M and k) are supposed to be fixed and tuned for best performance over the entire database, low amplitude means less samples are taken by the ADC. An example of such case is shown in Fig. 11(d) for Tape 222. Better results can be obtained if the amplitude of the input signals are tuned by using some kind of variable-gain amplifier, before applying to the ADC or using small values of k in the case of low-amplitude input signals. For example if the amplitude of the Tape 222 is multiplied by 1.5 before applying to the LC-ADC, the DER reduces from 8.1% to 2% for this tape.

It is possible to further improve the accuracy, but it requires additional circuits to adaptively adjust other parameters such as k and W, utilizing a search-back technique to recover the missed beats, or using sophisticated adaptive thresholding. All of them are at the expenses of higher complexity, power consumption and larger area. Since our target is for QRS detection in self-powered wearable device, the proposed algorithm strikes a balance between power and performance.

V. PERFORMANCE COMPARISON

In comparison to existing QRS-detection algorithms, the proposed one requires much less power. For a 7 bit LC-ADC and a gap of 4 LSB between the in-process quantization levels, the average sampling frequency is less than 67 Hz. By reducing the average sampling frequency, the activity of the system is minimized resulting significant reduction in dynamic power compared to the Nyquist sampling systems. In addition, as it is obvious from the algorithm operation, all the processing except the comparison of the two-bit data value with "00" and "11" and the timer operation, is done after a peak is detected. This reduces the processing rate from 67 Hz to less than 5 Hz, which is the average number of peaks per unit of time. In most of the conventional derivative-based algorithms, all of the subtractions and additions are performed for each sample and so the processing rate for these parts is equal to the sampling rate. Also as just 6 samples are needed for the detection, the memory requirement is lowest among all algorithms. Finally, the processing blocks involve only shift registers, adders, and comparators. No complex processing blocks such as multipliers are required. All these could lead to an ultra-low-power implementation of the proposed sampling-and-processing QRS-detection system. This is in contrast to many reported high-accuracy QRS-detection algorithms that utilize power-hungry complicated processing circuitries and abundant memory capacity [28], [29].

Although level-crossing sampling is used in [8] for the QRS-detection application, the LC-ADC in [8] does not utilize the increased value of k. Hence in [8] an analog filter is assumed to be employed before applying the signal to the ADC. Also adaptive thresholding is utilized in [8] in order to extract the critical features from the input signal, which may increase the power consumption in the implementation. In the proposed method, the

TABLE III
PERFORMANCE COMPARISON WITH OTHER QRS-DETECTION PROCESSORS

Ref.	Method	SE%	+P%	DER%	Area (mm^2)		Power (µW)		Technology	Supply voltage (V)	Simulation or Measurement
					ADC	Processor	ADC	Processor			
Zhang [16]	Mathematical Morphology	99.81	99.8	0.39	NA	NA	NA	2.7	0.35 µm	3.3	Simulation
Wang [30]	Pan-Tompkins	95.65	99.36	NA	NA	0.68	NA	2.21	0.18 µm	NA	Measurement
Ieong [28]	Quadratic Spline Wavelet Transform	99.31	99.7	0.99	0.096	1.11	2.36	0.83	0.35 µm	1.8	Measurement
Liu [31]	Discrete Wavelet Transform	99.8	99.86	0.35	NA	1.2	17.6	9	0.18 µm	1 - 1.1	Measurement
Min [32]	Wavelet-Based Detection	99.9	99.91	0.196	1.6	1.2	5.4	13.6	0.35 µm	3	Measurement
This work	Level-crossing Sampling	98.89	99.4	1.71	0.12	0.016	0.175	0.447	0.13 µm	1.2	Simulation

filtering function is embedded in detection process, which eliminates the use of extra filter for pre-processing. Also the proposed algorithm is simple in implementation and achieves acceptable performance over the entire MIT-BIH Arrhythmia Database. Table II shows the comparison of the proposed duration-based algorithm with the conventional amplitude-thresholding algorithm [8]. It can be seen that the proposed duration-based algorithm improves the detection performance for some of tapes.

To illustrate the low-power feature of the proposed algorithm, the proposed QRS detector including a 7-bit LC-ADC and the proposed duration-based QRS-detection algorithm was implemented in a 0.13 µm CMOS technology. The Synopsys Design Compiler is used for the synthesis of the LC-ADC and processor logics as well as power estimation. ECG signals from the MIT-BIH Arrhythmia Database are used as a test bench for generating switching activities in power estimation. The logic occupied area has been estimated using SoC Encounter. Simulations show that using a 5 kHz clock signal for the LC-ADC timer, and with a 1.2-V supply voltage, the LC-ADC and the processor consume 175 and 447 nW, respectively. The power consumption is dominated by leakage power, which can be further reduced by using low-power libraries. Without applying any low-power techniques, the power consumption of proposed system is much lower than conventional synchronous solutions, which are compared in Table III. Low power consumption and small area occupation of the proposed QRS-detection methodology make it suitable for body-area-network devices.

VI. CONCLUSION

A power-efficient asynchronous analog-to-information conversion system for QRS-detection application has been presented that contains a level-crossing ADC and a novel QRS-detection algorithm. It is shown that by reducing the processing rate to less than 5 Hz and using a few numbers of samples to make the decision, the system can be implemented with less complexity and less power consumption compared to the conventional regular-sampling synchronous systems. The system performance has been evaluated using the MIT-BIH Arrhythmia Database with a sensitivity of 98.89% and a positive prediction of 99.4%, without any filtering requirement. The performance of the proposed algorithm might be enhanced by applying techniques such as search-back and adaptive thresholding, at the cost of more power consumption.

REFERENCES

[1] J. Mark and T. Todd, "A nonuniform sampling approach to data compression," *IEEE Trans. Commun.*, vol. 29, no. 1, pp. 24–32, Jan. 1981.

[2] N. Sayiner, H. V. Sorensen, and T. R. Viswanathan, "A level-crossing sampling scheme for A/D conversion," *IEEE Trans. Circuits Syst. II, Analog Digit. Signal Process.*, vol. 43, no. 4, pp. 335–339, Apr. 1996.

[3] E. Allier, G. Sicard, L. Fesquet, and M. Renaudin, "A new class of asynchronous A/D converters based on time quantization," in *Proc. 9th IEEE Int. Symp. Asynchronous Circuits Syst.*, May 2003, pp. 196–205.

[4] E. Allier, J. Goulier, G. Sicard, A. Dezzani, E. Andre, and M. Renaudin, "A 120 nm low power asynchronous ADC," in *Proc. Int. Symp. Low Power Electron. Design*, Aug. 2005, pp. 60–65.

[5] M. Kurchuk and Y. Tsividis, "Signal-dependent variable-resolution clockless A/D conversion with application to continuous-time digital signal processing," *IEEE Trans. Circuits Syst. I, Reg. Papers*, vol. 57, no. 5, pp. 982–991, May 2010.

[6] K. Kozmin, J. Johansson, and J. Delsing, "Level-crossing ADC performance evaluation toward ultrasound application," *IEEE Trans. Circuits Syst. I, Reg. Papers*, vol. 56, no. 8, pp. 1708–1719, Aug. 2009.

[7] M. Trakimas and S. Sonkusale, "An adaptive resolution asynchronous ADC architecture for data compression in energy constrained sensing applications," *IEEE Trans. Circuits Syst. I, Reg. Papers*, vol. 58, no. 5, pp. 921–934, May 2011.

[8] R. Agarwal and S. Sonkusale, "Input-feature correlated asynchronous analog to information converter for ECG monitoring," *IEEE Trans. Biomed. Circuits Syst.*, vol. 5, no. 5, pp. 459–467, Oct. 2011.

[9] B. Schell and Y. P. Tsividis, "A continuous-time ADC/DSP/DAC system with no clock and with activity-dependent power dissipation," *IEEE J. Solid-State Circuits*, vol. 43, no. 11, pp. 2472–2481, Nov. 2008.

[10] Y. W. Li, K. L. Shepard, and Y. P. Tsividis, "A continuous-time programmable digital FIR filter," *IEEE J. Solid-State Circuits*, vol. 41, no. 11, pp. 2512–2520, Nov. 2006.

[11] Y. Hong, I. Rajendran, and Y. Lian, "A new ECG signal processing scheme for low-power wearable ECG devices," in *Proc. 2011 Asia Pacific Conf. Postgrad. Res. Microelectron. Electron. (PrimeAsia 2011)*, Oct. 2011, pp. 74–77.

[12] T. Wang, D. Wang, P. J. Hurst, B. C. Levy, and S. H. Lewis, "A level-crossing analog-to-digital converter with triangular dither," *IEEE Trans. Circuits Syst. I, Reg. Papers*, vol. 56, no. 9, pp. 2089–2099, Sep. 2009.

[13] E. Allier, G. Sicard, L. Fesquet, and M. Renaudin, "Asynchronous level crossing analog to digital converters," *Meas. J.*, vol. 37, pp. 296–309, Apr. 2005.

[14] F. Akopyan, R. Manohar, and A. B. Apsel, "A level-crossing flash asynchronous analog-to-digital converter," in *Proc. 12th IEEE Int. Symp. Asynchronous Circuits Syst.*, Grenoble, France, Mar. 2006, pp. 12–22.

[15] C. Weltin-Wu and Y. Tsividis, "An event-driven, alias-free ADC with signal-dependent resolution," in *Proc. 2012 IEEE Symp. VLSI Circuits Digest Tech. Papers*, Jun. 2012, pp. 28–29.

[16] F. Zhang and Y. Lian, "QRS detection based on multiscale mathematical morphology for wearable ECG devices in body area networks," *IEEE Trans. Biomed. Circuits Syst.*, vol. 3, no. 4, pp. 220–228, Aug. 2009.

[17] N. Arzeno, Z. Deng, and C. Poon, "Analysis of first-derivative based QRS detection algorithms," *IEEE Trans. Biomed. Eng.*, vol. 55, no. 2, pp. 478–484, Feb. 2008.

[18] Y. Wang, C. J. Deepu, and Y. Lian, "A computationally efficient QRS detection algorithm for wearable ECG sensors," presented at 33rd Annu. Int. Conf. IEEE EMBS (EMBC'2011), Boston, MA, USA, Aug. 30–Sep. 3.

[19] B. U. Köhler, C. Hennig, and R. Orglmeister, "The principles of software QRS detection," *IEEE Eng. Med. Biol. Mag.*, vol. 21, no. 1, pp. 42–57, Jan. 2002.

[20] A. Dixon, E. G. Allstot, D. Gangopadhyay, and D. J. Allstot, "Compressed sensing system considerations for ECG and EMG wireless biosensors," *IEEE Trans. Biomed. Circuits Syst.*, vol. 6, no. 2, pp. 156–166, Apr. 2012.

[21] G. Moody and R. Mark, "The impact of the MIT-BIH arrhythmia database," *IEEE Eng. Med. Biol.*, vol. 20, no. 3, pp. 45–50, May 2001.

[22] Physionet. (2013, Aug.). [Online]. Available: http://www.physionet.org/cgi-bin/atm/ATM

[23] A. L. Goldberger, L. A. Amaral, L. Glass, J. M. Hausdorff, P. C. Ivanov, R. G. Mark, J. E. Mietus, G. B. Moody, C. K. Peng, and H. E. Stanley, "PhysioBank, physiotoolkit, and physionet: Components of a new research resource for complex physiologic signals," *Circulation*, vol. 101, no. 23, pp. e215–e220, Jun. 2000.

[24] F. Aeschlimann, E. Allier, L. Fresquet, and M. Renaudin, "Asynchronous FIR filters: towards a new digital processing chain," in *Proc. 10th IEEE Int. Symp. Asynchronous Circuits Syst.*, Apr. 2004, pp. 198–206.

[25] F. Chiarugi, V. Sakkalis, D. Emmanouilidou, T. Krontiris, M. Varanini, and I. Tollis, "Adaptive threshold QRS detector with best channel selection based on a noise rating system," in *Proc. Comput. Cardiol.*, Sep. 2007, pp. 157–160.

[26] J. Pan and W. J. Tompkins, "A real-time QRS detection algorithm," *IEEE Trans. Biomed. Eng.*, vol. BME-32, no. 3, pp. 230–236, Mar. 1985.

[27] *Testing and Reporting Performance Results of Cardiac Rhythm and ST Segment Measurement Algorithms*, ANSI/AAMI EC57:1998/(R) 2008, Assoc. Advancement Med. Instrum. (AAMI), Arlington, VA, USA, 1998.

[28] C. I. Ieong, P. I. Mak, C. P. Lam, C. Dong, M. I. Vai, P. U. Mak, S. H. Pun, F. Wan, and R. P. Martins, "A 0.83-μW QRS detection processor using quadratic spline wavelet transform for wireless ECG acquisition in 0.35-μm CMOS," *IEEE Trans. Biomed. Circuits Syst.*, vol. 6, no. 6, pp. 586–595, Dec. 2012.

[29] N. Chaitanya, A. Radhakrishnan, G. Reddy, and M. Manikandan, "A simple and robust QRS detection algorithm for wireless medical body area networks," in *Proc. IEEE Int. Conf. Netw. Comput. Commun. (ETNCC2011)*, Apr., pp. 153–159.

[30] H. M. Wang, Y. L. Lai, M. C. Hou, S. H. Lin, B. S. Yen, Y. C. Huang, L. C. Chou, S. Y. Hsu, S. C. Huang, and M. Y. Jan, "A ±6 ms-accuracy, 0.68 mm^2 and 2.21 μW QRS detection ASIC," in *Proc. IEEE Int. Symp. Circuits Syst.*, 2010, pp. 1372–1375.

[31] X. Liu, Y. Zheng, M. W. Phyu, F. N. Endru, V. Navaneethan, and B. Zhao, "An ultra-low power ECG acquisition and monitoring ASIC system for WBAN applications," *IEEE J. Emerg. Sel. Topic Circuits Syst.*, vol. 2, no. 1, pp. 60–70, Mar. 2012.

[32] Y. J. Min, H. K. Kim, Y. R. Kang, G. S. Kim, J. Park, and S. W Kim, "Design of wavelet-based ECG detector for implantable cardiac pacemakers," *IEEE Trans. Biomed. Circuits Syst.*, vol. 7, no. 4, pp. 426–436, Aug. 2013.

Reza Lotfi (M'05) received the B.Sc. degree from Ferdowsi University of Mashhad, Mashhad, Iran, in 1997, the M.Sc. degree from Sharif University of Technology, Tehran, Iran, in 1999, and the Ph.D. degree in 2004 from University of Tehran, Tehran, Iran, all in electrical engineering.

From 2004 to 2010, he was an Assistant Professor with Ferdowsi University of Mashhad, Mashad, Iran, where he has been an Associate Professor since 2010. From 2008 to 2009, he was a Postdoctoral Scientific Researcher with Electronics Research Laboratory, Delft University of Technology, Delft, The Netherlands, where he was involved in ultra-low-power analog and mixed-signal integrated circuits for biomedical applications. His current research interests include low-voltage low-power analog integrated circuit design for biomedical microsystems as well as high-performance data converters.

Dr. Lotfi has been an Associate Editor of the IEEE TRANSACTIONS ON CIRCUITS AND SYSTEMS—I: REGULAR PAPERS since 2010.

Yong Lian (M'90–SM'99–F'09) received the B.Sc. degree from the College of Economics and Management, Shanghai Jiao Tong University, Shanghai, China, in 1984, and the Ph.D. degree from the Department of Electrical Engineering, National University of Singapore (NUS), Singapore, Singapore, in 1994.

He was with industry for nine years and joined the National University of Singapore in 1996, where he was the Deputy Department Head for Research, Area Director for IC and Embedded Systems, and Provost Professor in the Department of Electrical and Computer Engineering. Since 2013, he has been a Professor in Lassonde School of Engineering, York University. He is involved in teaching VLSI Digital Circuit Design, Integrated Digital Design, and Emerging Technologies in Electrical Engineering. He is the Founder of ClearBridge VitalSigns Pte. Ltd, a start-up for wireless wearable biomedical devices. His current research interests include biomedical circuits and systems and signal processing. He is the author or coauthor of more than 180 scientific publications in peer-reviewed journals, conference proceedings.

Dr. Lian is the recipient of the 1996 IEEE CAS Society's Guillemin-Cauer Award for the best paper published in the IEEE TRANSACTIONS ON CIRCUITS AND SYSTEMS II, the 2008 Multimedia Communications Best Paper Award from the IEEE Communications Society for the paper published in the IEEE TRANSACTIONS ON MULTIMEDIA, the winner of the 47th DAC/ISSCC Student Design Contest (as a Ph.D. Advisor), the Best Student Paper Award in the ICME'07 (as a M.Eng. Advisor), the 2011 IES Prestigious Engineering Achievement Award, and many other awards. He received 2009 and 2010 University Annual Teaching Excellent Awards and many other teaching awards in NUS. He is the Editor-in-Chief of the IEEE TRANSACTIONS ON CIRCUITS AND SYSTEMS II (TCAS-II), the Vice President for publications of the IEEE Circuits and Systems Society, Steering Committee Member of the IEEE TRANSACTIONS ON BIOMEDICAL CIRCUITS AND SYSTEMS (TBioCAS), the Past Chair of DSP Technical Committee of the IEEE Circuits and Systems (CAS) Society. He was an Associate Editors for the IEEE TCAS-I, TCAS-II, TBioCAS, and journal of Circuits, Systems, and Signal Processing (CSSP) for more than 10 years, and was the Guest Editor for 8 Special Issues in TCAS-I, TBioCAS, and CSSP. He was the Vice President for Asia Pacific Region of the IEEE CAS Society from 2007 to 2008, AdComm Member of the IEEE Biometrics Council (2008–2009), CAS Society Representative to the BioTechnology Council (2007–2009), the Chair of the BioCAS Technical Committee of the IEEE CAS Society (2007–2009), the Member of the IEEE Medal for Innovations in Healthcare Technology Committee (2010–2012), and the Distinguished Lecturer of the IEEE CAS Society (2004–2005). He is the Founder of the International Conference on Green Circuits and Systems (ICGCS), Asia Pacific Conference on Postgraduate Research in Microelectronics and Electronics (PrimeAsia), and the IEEE Biomedical Circuits and Systems Conference (BioCAS). He is a Fellow of the Academy of Engineering Singapore.

Nassim Ravanshad (S'07) was born in Mashhad, Iran in 1984. She received her B.S. and M.S. degrees in electrical engineering in 2006 and 2008, respectively, from Ferdowsi University of Mashhad, Mashhad, Iran, where she is currently working toward the Ph.D. degree.

Her current research interests include design of analog and mixed-signal integrated circuits and systems, data converters, and biomedical circuits and systems.

Hamidreza Rezaee-Dehsorkh (S'07) was born in Mashhad, Iran, in 1983. He received the B.S. and M.S. degrees in electrical engineering in 2006 and 2008, respectively, from Ferdowsi University of Mashhad, Mashhad, Iran, where he is currently working toward the Ph.D. degree.

His current research interests include design of analog and mixed-signal integrated circuits and systems, data converters, and biomedical circuits and systems.